

03.02.02.45: ICE: Energy Efficiency Improvement Approaches in Ice Related Processes



Praveen Cheekatamarla
Hongbin Sun

February 2023

DOCUMENT AVAILABILITY

Reports produced after January 1, 1996, are generally available free via US Department of Energy (DOE) SciTech Connect.

Website www.osti.gov

Reports produced before January 1, 1996, may be purchased by members of the public from the following source:

National Technical Information Service
5285 Port Royal Road
Springfield, VA 22161
Telephone 703-605-6000 (1-800-553-6847)
TDD 703-487-4639
Fax 703-605-6900
E-mail info@ntis.gov
Website <http://classic.ntis.gov/>

Reports are available to DOE employees, DOE contractors, Energy Technology Data Exchange representatives, and International Nuclear Information System representatives from the following source:

Office of Scientific and Technical Information
PO Box 62
Oak Ridge, TN 37831
Telephone 865-576-8401
Fax 865-576-5728
E-mail reports@osti.gov
Website <https://www.osti.gov/>

This report was prepared as an account of work sponsored by an agency of the United States Government. Neither the United States Government nor any agency thereof, nor any of their employees, makes any warranty, express or implied, or assumes any legal liability or responsibility for the accuracy, completeness, or usefulness of any information, apparatus, product, or process disclosed, or represents that its use would not infringe privately owned rights. Reference herein to any specific commercial product, process, or service by trade name, trademark, manufacturer, or otherwise, does not necessarily constitute or imply its endorsement, recommendation, or favoring by the United States Government or any agency thereof. The views and opinions of authors expressed herein do not necessarily state or reflect those of the United States Government or any agency thereof.

Buildings and Transportation Sciences Division

**ENERGY EFFICIENCY IMPROVEMENT APPROACHES IN ICE RELATED
PROCESSES**

Praveen Cheekatamarla
Hongbin Sun

February 2023

Prepared by
OAK RIDGE NATIONAL LABORATORY
Oak Ridge, TN 37831-6283
managed by
UT-BATTELLE LLC
for the
US DEPARTMENT OF ENERGY
under contract DE-AC05-00OR22725

CONTENTS

CONTENTS.....	iii
EXECUTIVE SUMMARY	6
1. OBJECTIVE.....	6
2. APPROACH.....	6
3. MATERIALS AND PROCESSES.....	7
4. RESULTS AND DISCUSSION.....	12
5. CONCLUSIONS	26

TABLE OF FIGURES

Figure 1: Typical forces in action during any ice harvesting process.....	6
Figure 2: Schematic of the test setup to measure the ice adhesion strength on a test sample.....	7
Figure 3: Sheet metal coupons with precise surface area for ice formation.	7
Figure 4: Ice adhesion strength measurement using a 110 lbf force gauge	8
Figure 5: Force probe height adjustment to measure mixed tensile-shear forces on the ice layer.....	8
Figure 6: Integrated test setup for measuring ice adhesion strength on different substrates.....	8
Figure 7: Separation of the ice column from the substrate via force probe.	9
Figure 8: Peak force measurement – screenshot of the force measurement software	9
Figure 9: Ice column formation with a secured hook for measuring normal stress	9
Figure 10: Integrated force gauge and freezer test setup to measure normal stress on the ice column adhered to the sheet metal coupon.	10
Figure 11: Ice adhesion strength measurement of tubular substrates – test sample.....	11
Figure 12: Load cell for measuring the ice adhesion strength of tubular substrates.....	11
Figure 13: Screenshot of the force gauge measuring the ice adhesion strength on tubular substrates.....	12
Figure 14: Force to remove an untreated copper tube from an ice column.	12
Figure 15: Force measurement to remove Enhanced copper tubes from the ice column.	13
Figure 16: 3/8” OD SS 304 (untreated) tube in contact with ice formed at -5°F.	13
Figure 17: 3/8” OD SS 304 (Enhanced) tube in contact with ice formed at -5°F and 15°F.	13
Figure 18: Shear force application on ice (formed at 5°F) contact between Enhanced and untreated SS304 sheet metal.	14
Figure 19: Tensile force application on ice (formed at -5°F) contact between Enhanced and untreated copper sheet metal.....	14
Figure 20: Shear force application on ice formed at 20°F on Enhanced and untreated copper sheet metal - time to dislodge the ice.	15
Figure 21: Force measurement on different copper (untreated) tubes in contact with ice formed at -5°F.	16
Figure 22: Force measurement on different copper (Enhanced) tubes in contact with ice formed at -5°F.	16
Figure 23: Force measurement on 3/8” OD SS 304 (untreated) tube in contact with ice formed at - 5°F.....	17
Figure 24: Force measurement on 3/8” OD SS 304 (Enhanced) tube in contact with ice formed at -5°F.	17
Figure 25: Untreated Aluminum tube in contact with ice formed at -5°F. 3/8” OD.....	18
Figure 26: Force measurement on Enhanced aluminum tube in contact with ice formed at -5°F.....	18
Figure 27: Test setup to study the influence of induced energy on ice dislocation from the substrate	19
Figure 28: Ice structure formation on different surfaces with the transducer collocated underneath.....	19
Figure 29: Customized metal structure to investigate energy propagation.....	20
Figure 30: A compilation of videos showing the efficacy of ice removal from different surfaces.....	20
Figure 31: Laser vibrometer to measure the resonant frequency of ice molds	21
Figure 32: Diagram of the experimental setup for the vibration measurement using laser Doppler vibrometer (left) and testing system (right)	21
Figure 33: Round ice cube tray with 40 kHz ultrasonic transducer (top), and the measurement points on the front surface.....	22
Figure 34: Displacements at the REF excited at five power levels	23
Figure 35: Commercial ice cube tray with a PZT plate (top) and measurement locations (bottom).....	23

Figure 36: Displacement response at C4 when sweeping from 25 kHz to 100 kHz.....	24
Figure 37: Displacements map for the ice tray with one PZT on the top side surface (excitation frequency: 54 kHz)	24
Figure 38: Displacements map for the ice tray with three PZT on the top, left, and right-side surfaces (excitation frequency: 54 kHz).	25
Figure 39: Force measurement on enhanced and as-received copper tubes in contact with ice formed at 7°F	25

TABLE OF TABLES

Table 1 Displacement (unit: nm) at the 18 positions with 40 kHz and 5W excitation.....	22
---	----

EXECUTIVE SUMMARY

A detailed survey of ice mold and evaporator metal surfaces, physical structures, operational conditions, materials of construction, design of different equipment was reviewed and analyzed¹. A reliable test methodology was developed to measure the ice adhesion strength of different materials and geometries identified. The developed test setup was successfully employed in measuring the ice adhesion strength on both tubular and planar substrate geometries of metals including copper, aluminum, stainless steel. Application of advanced polymer materials in lowering the adhesion strength of ice was confirmed where the measured strength was lowered by 50-70% depending on the material and geometry. Additionally, utilization of induced ultrasonic vibration in further lowering the ice harvesting energy was confirmed on multiple materials and geometries. Durability of the coating enhancement was also confirmed in a thermal cycling test under realistic operating conditions.

1. OBJECTIVE

The primary objective of this project is to develop an energy efficient methodology to dispense ice from the ice maker mold. Ice is an important commodity both as a direct use product and as a nuisance in day-to-day refrigeration related equipment. It is utilized: as an energy storage medium at industrial scale, in the food service industry, in domestic household refrigeration, and in supermarkets. Ice making is an energy intensive process, where ~ 30% of this energy is exclusively consumed during the dispensing process which involves mold heating for dislodging the ice followed by re-cooling of the thermal mass to attain the desired temperature for the subsequent cycle. The key objective of this project was to help dislocate the ice layer using advanced materials and ultrasonic vibration to lower ice adhesion strength.

2. APPROACH

A test setup was developed to evaluate the amount of force necessary to dislodge the ice layer contacting the substrate material being investigated. A standardized methodology to reliably compare the energy intensity values on different surfaces including the ones with enhancements is the key towards developing the desired material for lowering the adhesion strength of ice. Typical forces that are bound to occur during the ice making process include shear, tensile and mixed forces, as shown in the Figure 1 below.

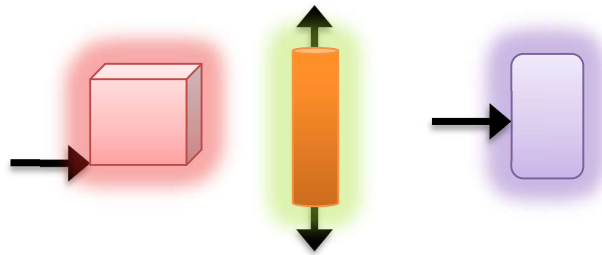


Figure 1: Typical forces in action during any ice harvesting process

The ability to measure these forces in a precise and reliable manner requires a reliable method to impose each of these forces while being able to detect the peak force at the time of separation of the ice interfacial layer from the substrate. A schematic of the test setup at the beginning of this effort is

¹ Cheekatamarla, P. (2022). *Materials and methods used in the ice making process* (No. ORNL/TM-2021/2350). Oak Ridge National Lab.(ORNL), Oak Ridge, TN (United States).

shown in Figure 2. Key aspects of such a method must include a high-resolution force meter, ice structure formation on the substrate, temperature control of the ice structure and the substrate, ability to move the force gauge at a fixed speed (motorized, controlled force exertion), peak force measurement, and the ability to exert force in different directions.

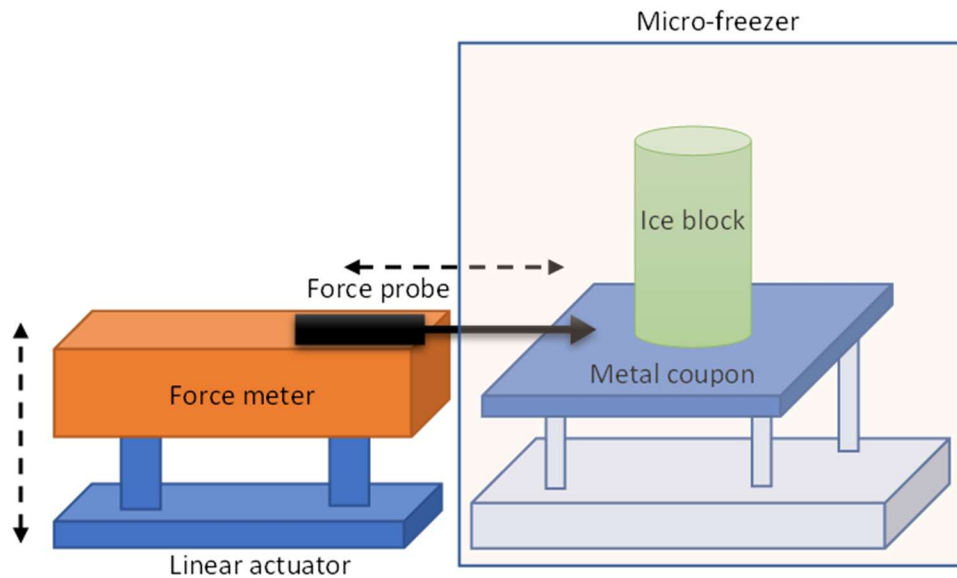


Figure 2: Schematic of the test setup to measure the ice adhesion strength on a test sample.

Integration of the cold test sample and the load cell for precisely measuring the adhesion strength of ice on substrates requires controlled contact surface area. Experimental setup to accomplish such a measurement of all potential (shear, tensile and mixed) forces on sheet metal coupons and tubes has been designed, as described below.

3. MATERIALS AND PROCESSES

Figure 3 shows the test methodology adopted for making repeatable ice column structures with fixed surface contact area. The sheet metal coupon is affixed with a precise boundary of wax layer to contain the ice formation in a 29 mm opening in the wax sheet. This allows for repeatable structure formation in a plastic tube, where the only contact point is restricted to the 29 mm circle.

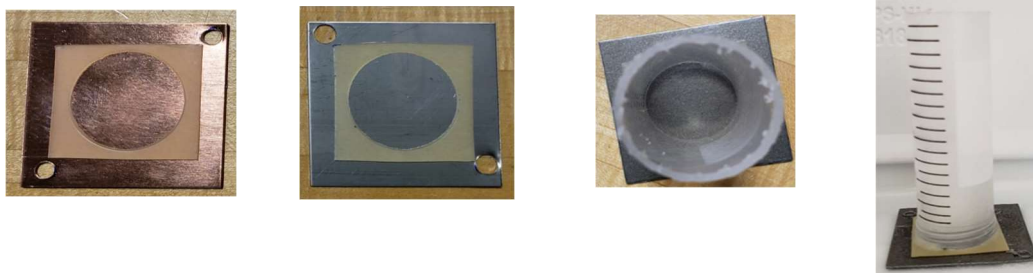


Figure 3: Sheet metal coupons with precise surface area for ice formation.

Formation of ice structure is accomplished insitu in the -20 deg F refrigerator where the test sample is loaded and secured. A thin layer of water is initially deposited inside the plastic tube for the solid ice layer to form. Ice-cold water maintained at a temperature of 36 deg F in a separate refrigerator is then poured on top of the initial ice layer and allowed to freeze for > 60 minutes. The load cell containing a horizontal motion stand capable of moving the 110 lbf force gauge (IMADA, ZTA-110, ZTA-220) at 1 - 300 mm/min (MH2-550) is connected via a small opening in the wall of the refrigerator. This allows free movement of the force probe without any obstruction, as shown in Figure 4.

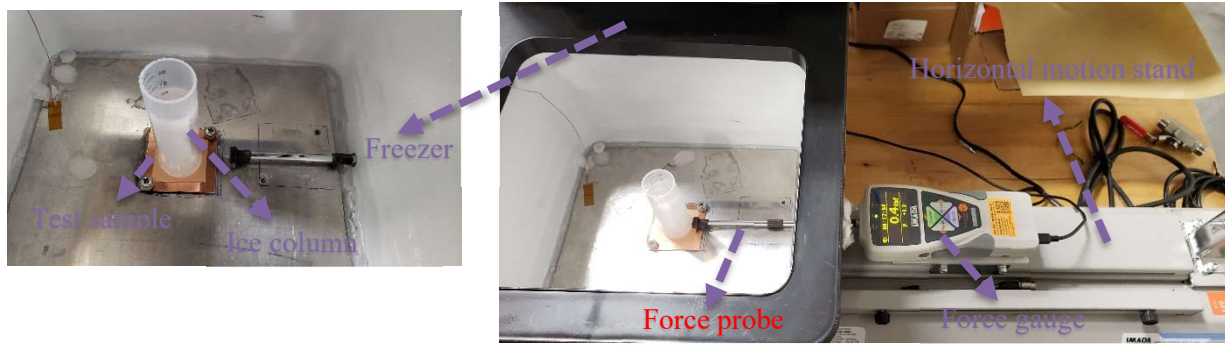


Figure 4: Ice adhesion strength measurement using a 110 lbf force gauge

As shown in Figure 4, shear force measurement is accomplished by exerting the force probe at the base of the ice column. However, adjusting the height of the probe along the axis of the ice column also allows for mixed force measurement where tensile forces are prevalent, as shown in Figure 5.



Figure 5: Force probe height adjustment to measure mixed tensile-shear forces on the ice layer

Figure 6 shows the complete test setup with the freezer and force meter connected. Also shown is the control panel of the motion test stand with adjustable speed. Figure 7 shows a picture immediately after dislodging the ice column from the substrate.



Figure 6: Integrated test setup for measuring ice adhesion strength on different substrates



Figure 7: Separation of the ice column from the substrate via force probe.

Figure 8 shows a screenshot of the force measurement as a function of time. As can be seen, the peak force is recorded at the moment the ice is dislodged from the surface. This allows for precise measurement and comparison under identical operational environment on different substrates.



Figure 8: Peak force measurement – screenshot of the force measurement software

A similar test procedure was also developed for exerting vertical/tensile force on the ice column to measure the adhesion strength on both sheet metal coupons and tubular structures. Ability to pull the entire ice column from the substrate along the axis is accomplished through a hook inserted in the water before freezing in place, as shown in Figure 9. The hook is initially supported on the rim of the plastic tube perpendicularly before beginning the freezing process. The formation of ice around the hook rod and supporting nut/washer arrangement in the bottom ensure secure contact throughout the surface, much stronger than the 29 mm circular contact area on the substrate. As a result, exertion of a force normal to the substrate allows dislodging of the ice column from the sheet metal coupon first, allowing the measurement of the tensile force.



Figure 9: Ice column formation with a secured hook for measuring normal stress

The test sample shown in Figure 10 was then secured to the 1/8" thick aluminum sheet metal affixed to the base of the freezer measuring 120 in² surface (with ice as well as heavy duty double sided sticky tape). The amount of force to be measured on the 29 mm surface is much smaller than what is required to remove the base plate, hence the force measurement by the gauge is an accurate representation of the ice adhesion strength of the substrate. Figure 3.8 shows the complete test setup, where a 1.5" hole on the lid of the freezer allows the connection with the force probe via a hook. The probe is lowered gently to not exert any force and carefully connected to the hook of the ice column. The top lid is then sealed with insulation and allowed to sit for at least 60 minutes before pulling the probe upwards to measure the peak force.



Figure 10: Integrated force gauge and freezer test setup to measure normal stress on the ice column adhered to the sheet metal coupon.

Measurement of the ice adhesion strength on tubular structures was addressed using a similar approach as above but with the ability to pull the tube out of the ice. As shown in Figure 11, the test sample (PTFE tube shown) is secured to a compression fitting on one side and a bolt ring on the opposite side. This fixture is then inserted into a cylindrical vessel filled with water. The entire structure is allowed to freeze for at least 60 minutes before transferring to the force measurement test stand. The exact length and diameter of the tube is measured prior to inserting in the water. Top edge of the vessel is ensured to not have any water to avoid adhesion of the support ring underneath the compression fitting. It must be noted that any exertion of force normal to the surface hence acts only on the tubular surface. The ice contact surface was controlled by sealing the open end of the tube with wax. These precautions allowed precise measurement of the adhesion strength per unit surface area of the tubular substrate.



Figure 11: Ice adhesion strength measurement of tubular substrates – test sample

Figure 12 shows the force probe attached to the tubular test sample adhered to the ice layer throughout its surface. An external container filled with ice surrounding the test sample was used to ensure minimal heat gain by the test substrate for each measurement. This minimized errors in the measured adhesion strength values.



Figure 12: Load cell for measuring the ice adhesion strength of tubular substrates

Figure 13 displays a sample screenshot of the ice adhesion strength on tubular structure. It can be noticed that the measured value is negative since the force probe is pulled away rather than force exertion via pushing on the substrate.

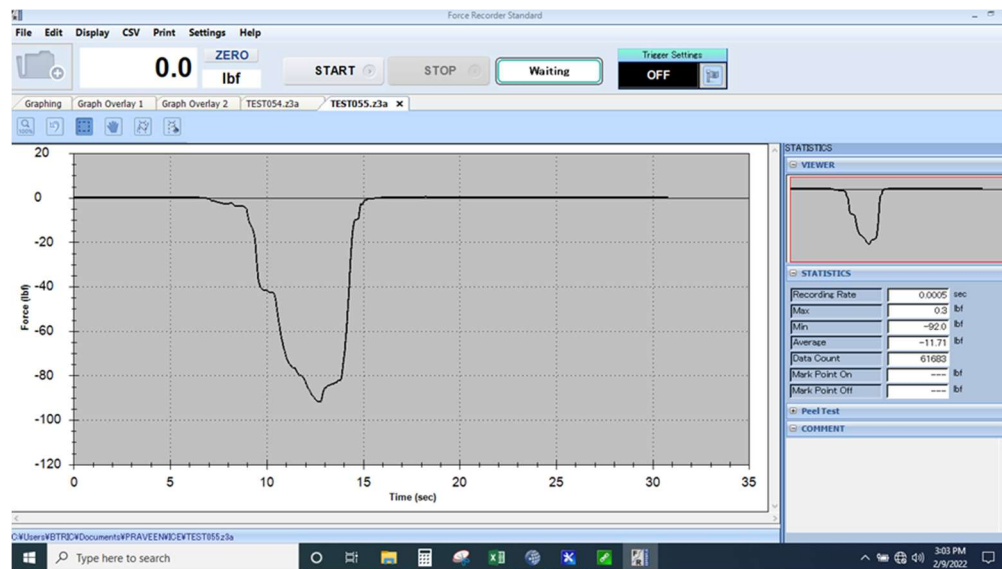


Figure 13: Screenshot of the force gauge measuring the ice adhesion strength on tubular substrates

4. RESULTS AND DISCUSSION

4.1: Effectiveness of the coating enhancement

Ice adhesion strength measurements on different geometries and substrate metals were conducted. The test setup described in section 3 above was employed in evaluating the force necessary to dislodge the ice from the underlying substrate metal. Shear, tensile, and normal forces were measured on virgin and icephobic material treated sheet metal and tubular structures. Figure 14 and Figure 15 below show the influence of enhancement in lowering the force necessary to pull out the tube from the ice column, simulating the ice harvesting mechanism typically utilized in ice makers. A 0.375" diameter as received, cleaned copper tube was evaluated first (shown below) demonstrating ~ 44 lbf needed to separate the tube from the ice.

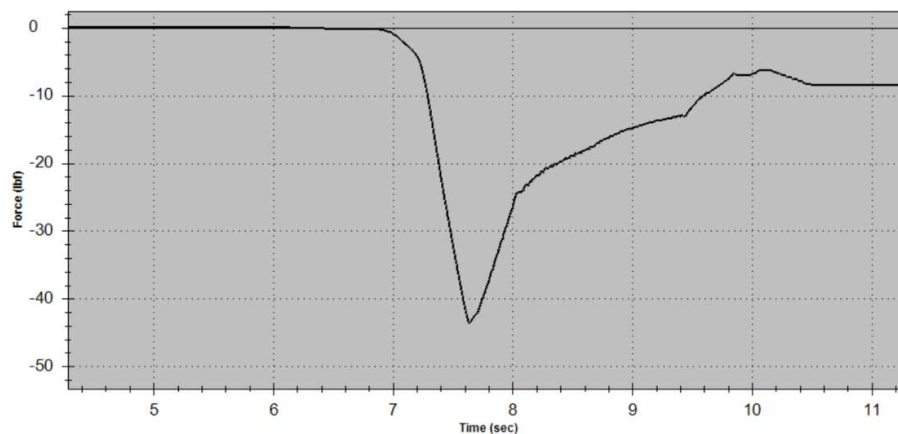


Figure 14: Force to remove an untreated copper tube from an ice column.

Enhancement with the surface with icephobic material on two separate copper tubes lowered the force to ~ 19 to 22.5 lbf, as shown in Fig. 4.2 below.

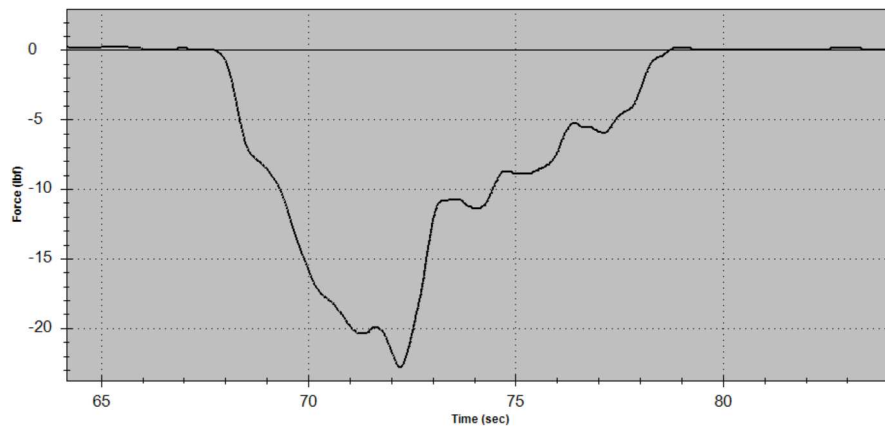


Figure 15: Force measurement to remove Enhanced copper tubes from the ice column.

The tests were also repeated for stainless steel tubes measuring 3/8" OD. As received tubing was cleaned first, followed by tubular ice structure formation at -5°F. Ice separation force was measured at ~ 63 lbf on an untreated tube (Figure 16).

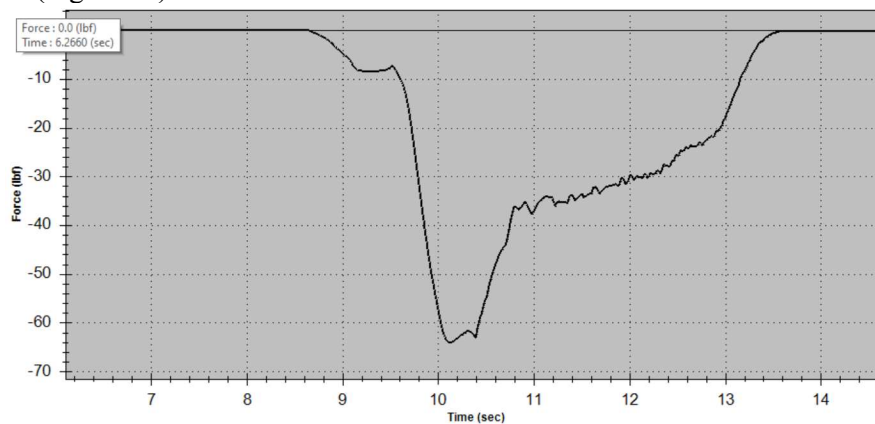


Figure 16: 3/8" OD SS 304 (untreated) tube in contact with ice formed at -5°F.

The tests were repeated for similar stainless tubes enhanced with the coating. Figure 17 displays the measured force necessary to separate the tube from the ice structure formed at two different temperatures, -5°F and 15°F. As shown, compared to the untreated surface, the enhanced tubes demonstrated lower force of ~ 31 lbf for ice separation.

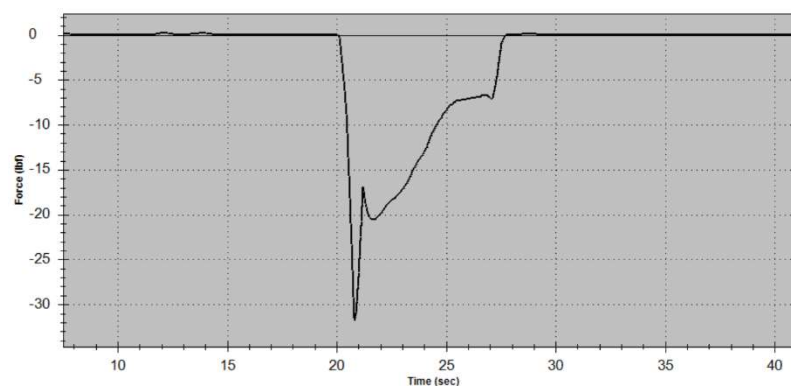


Figure 17: 3/8" OD SS 304 (Enhanced) tube in contact with ice formed at -5°F and 15°F.

Measurements of the shear force necessary to separate the ice column from copper sheet metal with and without enhancement showed that the dislodging force decreased significantly (not shown) compared to the untreated surface, similar to the results noticed on tubular structures.

Figure 18 shows the force measured on a stainless steel (304) coupon with and without enhancement. The untreated surface required ~ 5 lbf to dislodge the ice whereas two separate enhanced samples showed a peak force of ~ 3 lbf. The speed of the horizontal motion test stand was set at 50 mm/min during this test. During the process of ice separation from the metal surface, the column can obstruct the force probe motion and offers further resistance even after ice separation. Consequently, as shown in the figure, for the Enhanced samples, the measured force is above zero even after detecting the peak value.

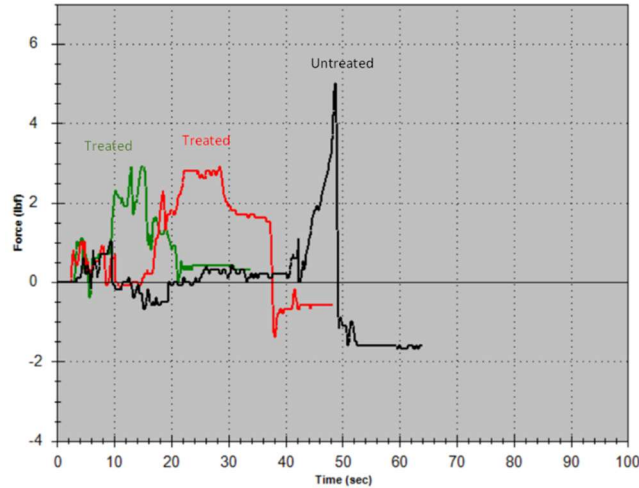


Figure 4.5

Figure 18: Shear force application on ice (formed at 5°F) contact between Enhanced and untreated SS304 sheet metal.

This behavior was corrected by increasing the speed of the force probe to 300 mm/min and decreasing the ice contact surface area from 0.8 in² to 0.4 in², allowing the ice column to completely move away from the force probe. As a result, the measured force values were repeatable on a copper sheet metal coupon and showed similar force vs. time profile during all the tests conducted.

Evaluation of ice adhesion strength on copper sheet metal was also performed using the tensile force measurement test bench described in the milestone report. A copper sheet metal coupon was evaluated by forming the ice column at 5°F according to the procedure described earlier. Figure 19 shows the influence of enhancement in lowering the force necessary to disconnect the ice layer from the surface of the substrate.

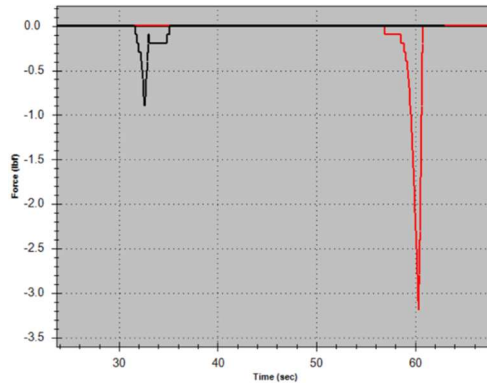


Figure 19: Tensile force application on ice (formed at -5°F) contact between Enhanced and untreated copper sheet metal.

In addition to evaluating the impact of LIT materials on adhesion strength of ice, the time necessary to dislodge the ice was also investigated. Figure 20 shows a comparison of the force versus time curves of copper sheet metal where shear forces were measured with and without enhancement. On the untreated surface, the peak force was realized at ~0.9 seconds after exerting the initial force whereas the enhanced surface shortened this time to ~0.3 seconds.

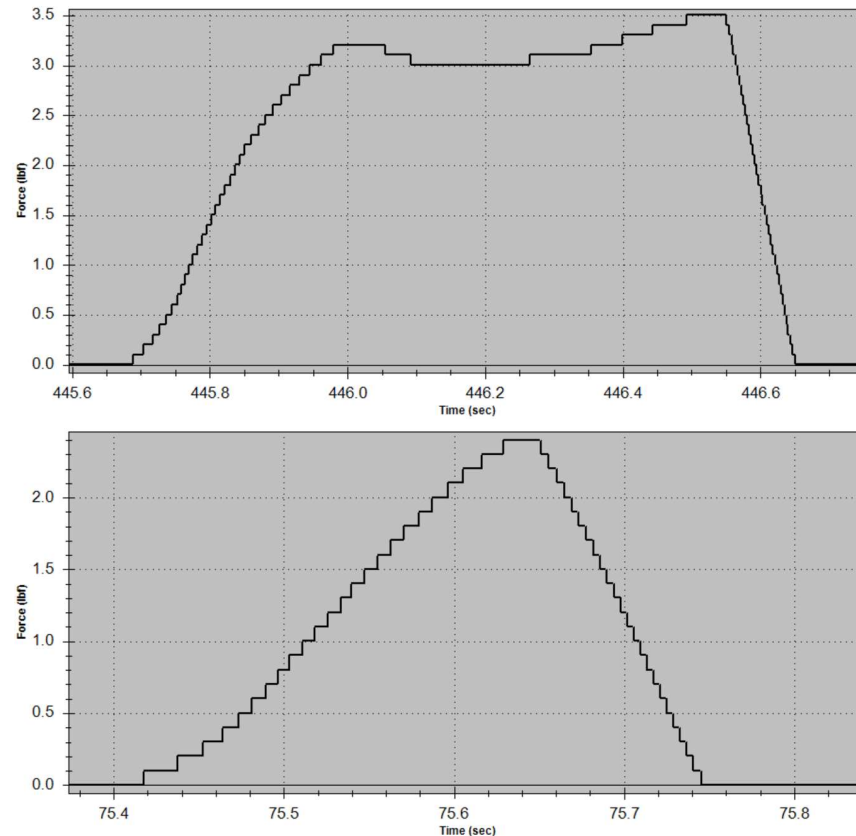


Figure 20: Shear force application on ice formed at 20°F on Enhanced and untreated copper sheet metal - time to dislodge the ice.

Force vs time measurements were also repeated for SS304 sheet metal surfaces with and without enhancement. The untreated surface required 0.6 seconds to attain the peak force whereas the enhanced surface required ~0.2 seconds.

Repeatability of the noticed reduction in ice adhesion strength on copper tube was studied by subjecting each tube to tensile test for dislodging from the ice column formed at -5°F. Figure 21 shows the peak force measured on copper tubes in the range of 55 lbf to 62 lbf.

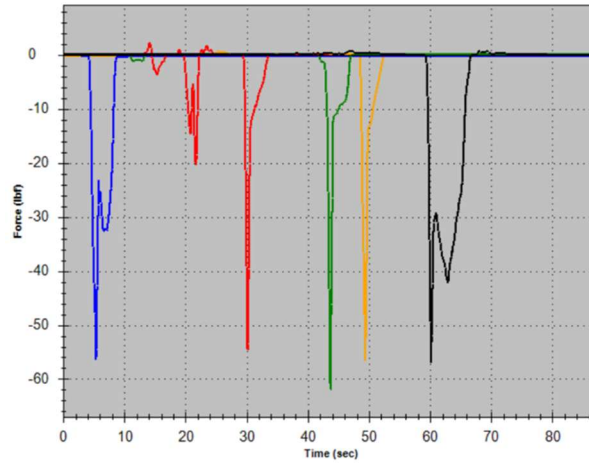


Figure 21: Force measurement on different copper (untreated) tubes in contact with ice formed at -5°F .

Compared to the untreated surface, enhanced copper tubes showed significant decrease in peak force necessary to dislodge the ice column. As shown in Figure 22, the enhanced tubes needed the peak force in the range of 23-25 lbf.

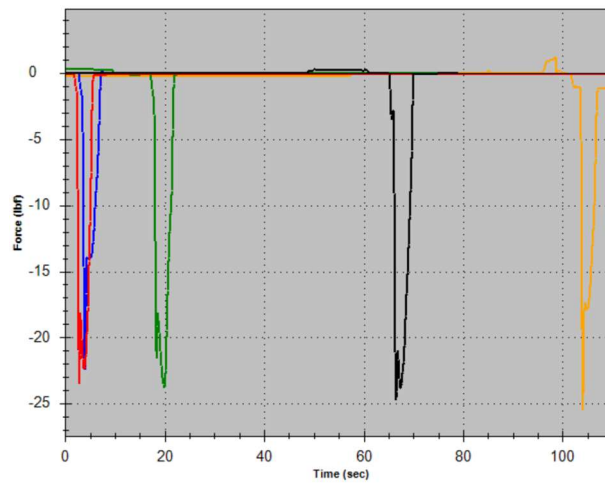


Figure 4.9:

Figure 22: Force measurement on different copper (Enhanced) tubes in contact with ice formed at -5°F .

Similarly, repeatability of the measured peak force on stainless steel tubes were also studied for untreated and enhanced surfaces. Figure 23 and Figure 24 display the peak force at ~ 66 lbf, and ~ 34 lbf for untreated and enhanced surfaces respectively.

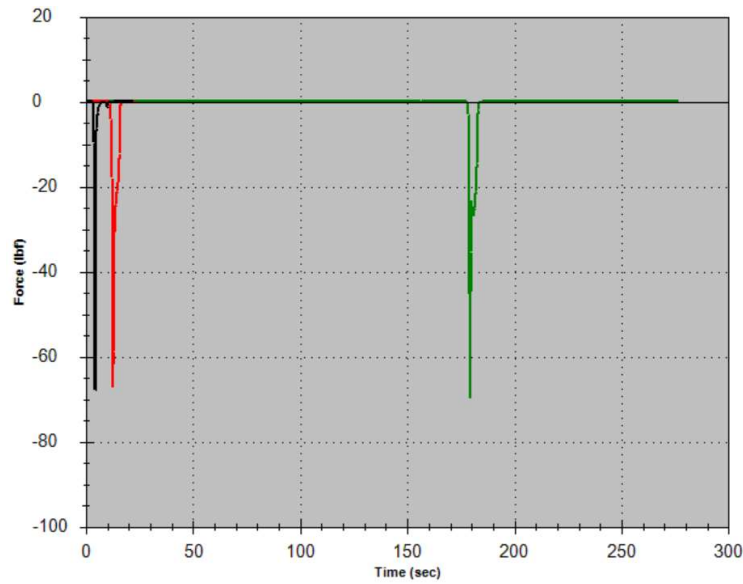


Figure 23: Force measurement on 3/8" OD SS 304 (untreated) tube in contact with ice formed at -5°F.

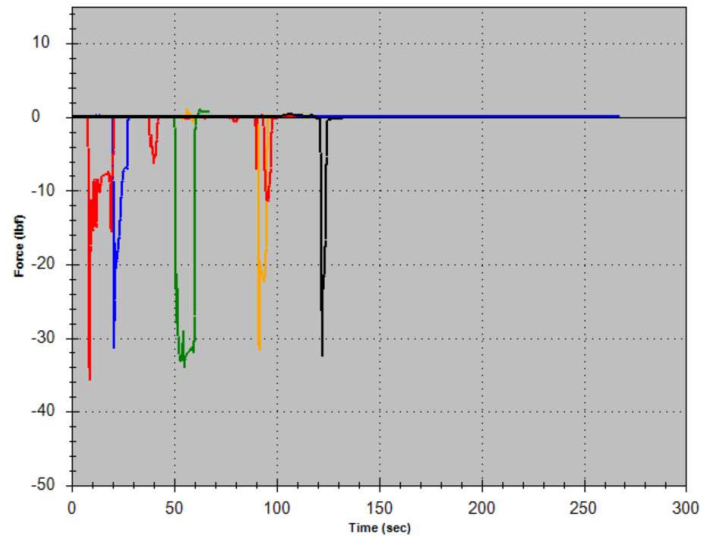


Figure 24: Force measurement on 3/8" OD SS 304 (Enhanced) tube in contact with ice formed at -5°F.

Similarly, aluminum tubes also showed repeatable behavior where the untreated tubes required ~42 lbf (Figure 25), whereas Enhanced tubes showed a decrease in the peak force value at ~ 22 lbf (Figure 26).

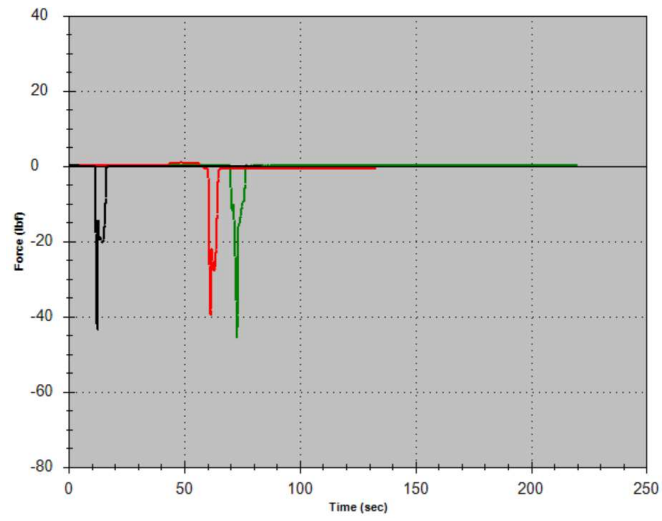


Figure 25: Untreated Aluminum tube in contact with ice formed at -5°F. 3/8" OD.

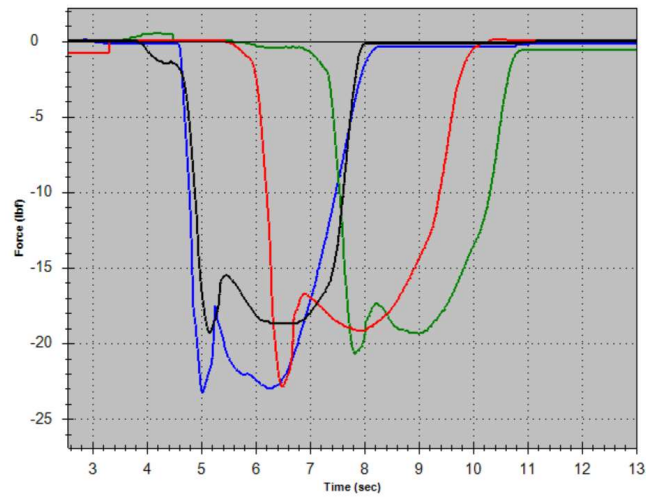


Figure 26: Force measurement on Enhanced aluminum tube in contact with ice formed at -5°F.

4.2 Influence of Induced Energy

Application and efficient utilization of induced energy to minimize the energy consumption during ice harvesting process was targeted via ultrasonic vibration of the substrate. A test facility to form ice insitu inside a freezer capable of cooling down to -4°F and integrated with ultrasonic transducers capable of generating 40 kHz frequency was designed and built, as shown in Figure 27 below.

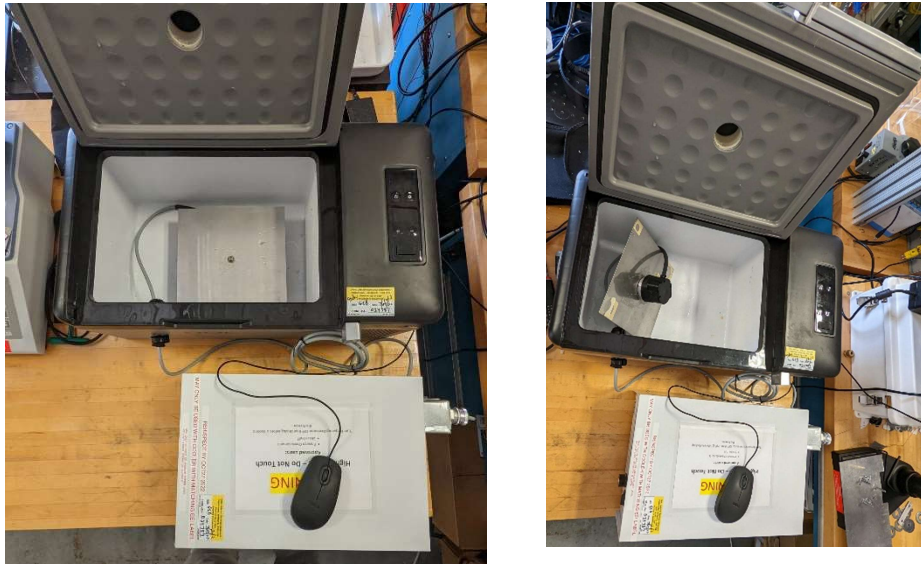


Figure 27: Test setup to study the influence of induced energy on ice dislocation from the substrate

This test setup allowed formation of different ice structures on various metals and substrates while in direct contact with the active surface of the ultrasonic transducer. Activation of the transducer allowed visualization of the deicing process and the ability to measure time constant for achieving interfacial surface fracture and separation from the cold substrate. Sheet metal measuring 2" to 8" were installed with a 1.5" diameter langevin type transducers as shown in Figure 28 below. Experiments were conducted to study the impact of ultrasonic frequency on dislodging the ice from the underlying substrate.



Figure 28: Ice structure formation on different surfaces with the transducer collocated underneath

The test setup reported above was utilized for evaluating different metals, substrates, ice structures, and geometries to identify the influence of externally induced energy in fracturing the interfacial layer between ice and metal surface. Ice in the form of sheet, cubes, spheres etc. were all formed on structures measuring up to 10” wide and subjected to excitation at a fixed frequency of 40 kHz. The fracturing mechanism remained effective irrespective of the surface contact as well as the ability to propagate the ultrasonic frequency over long distances of up to 6”, as shown in the custom-built metal structure below (Figure 29).

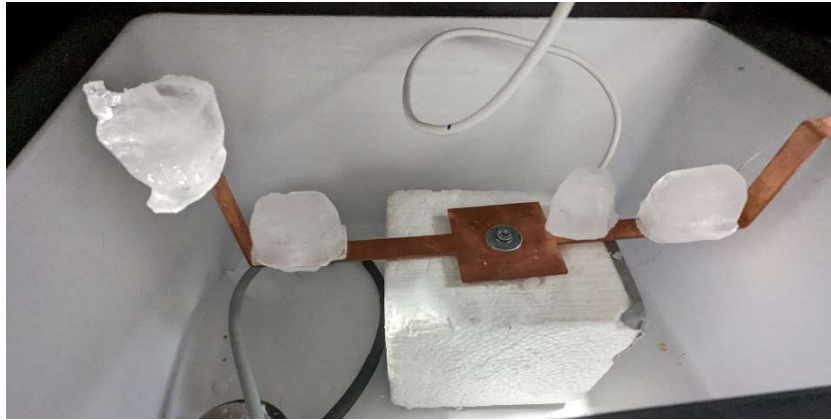


Figure 29: Customized metal structure to investigate energy propagation

The primary objective of this structure was to see if a central source of induced energy is sufficient to excite and dislodge an ice structure formed at a distance. The overall approach of induced energy to fragment the interface was shown to be effective. Results from these studies are shown in the video below.



PXL_20220711_1644
16636_TS_3_AdobeEx

Double click this icon

Figure 30: A compilation of videos showing the efficacy of ice removal from different surfaces

It is important to understand the influence of the frequency and energy supplied to optimize the resonance of the evaporator under investigation. Hence, a laser vibrometer was investigated as potential tool to measure the resonant frequency using a frequency generator and amplifier, as shown in Figure 31 below.

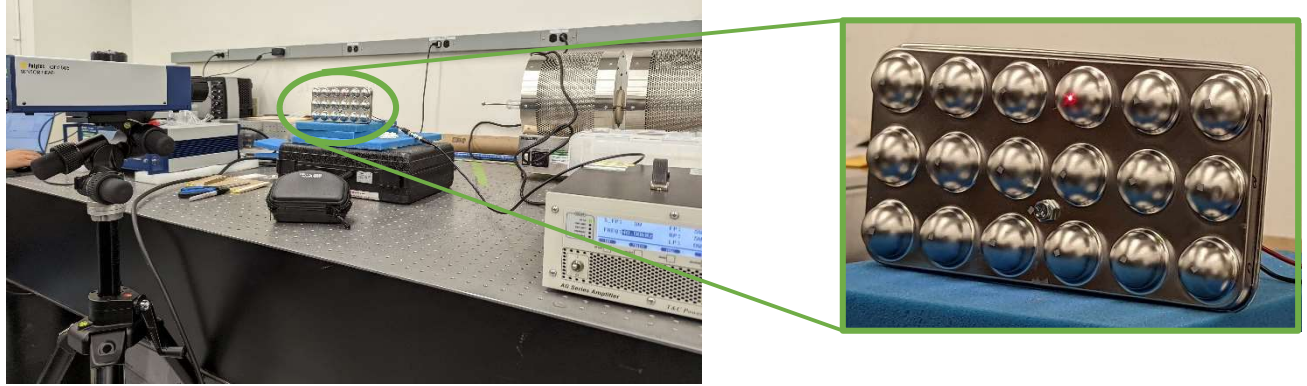


Figure 31: Laser vibrometer to measure the resonant frequency of ice molds

Measurement of vibration using the laser Doppler vibrometer: The setup of the vibration measurement is shown in Figure 32. An ultrasonic actuator is installed on the ice tray with a bolt or permanent epoxy. A function generator and RF amplifier are used to excite the ultrasonic actuator. The vibration of the test panel is measured using a laser Doppler vibrometer (LDV, Polytech, OFV 505). The vibration signal is digitized by the oscilloscope first and then saved at the computer.

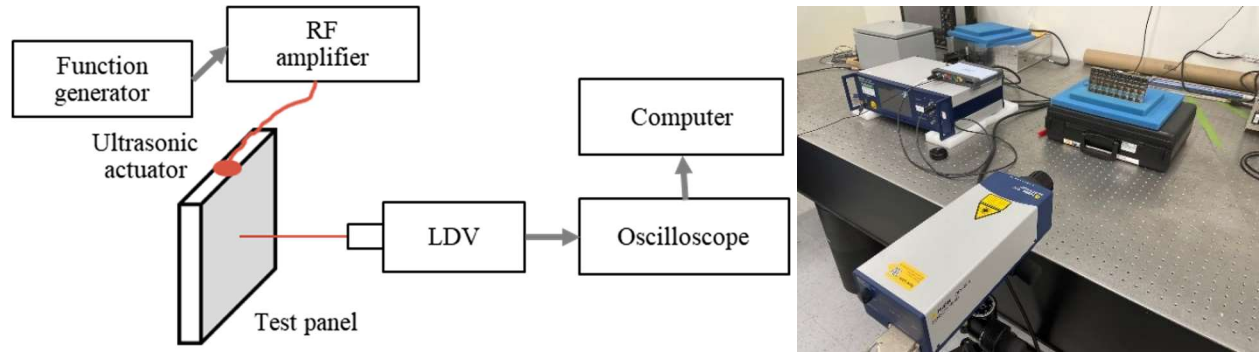


Figure 32: Diagram of the experimental setup for the vibration measurement using laser Doppler vibrometer (left) and testing system (right)

The direct output from the LDV is the voltage history with a velocity decoder. In order to convert the maximum voltage to maximum displacement, the following equation is used assuming a harmonic vibration:

$$u_{max} = V_{out,max} * \delta / \omega. \quad (1)$$

Here, $V_{out,max}$ is the maximum voltage output, δ is the sensitivity of the velocity decoder (50 mm/s/V used in this work), and ω is the angular frequency of the excitation.

(a) Round ice cube tray

A trial test was conducted on a round ice cube panel using a 40 kHz ultrasonic transducer (see Figure 33). An ultrasonic amplifier (AG1014, T&C Power Conversion, Inc.) with a power range of 5W to 20W at the

frequency of 40kHz was used, which was the working frequency of the selected model. On the front surface, reflective tapes for the LDV were glued on the measurement points ($3 \times 6 = 18$ points). The ultrasonic transducer was installed between B3 and C4 with a bolt. Table 1 shows the absolute displacements of the 18 points and a reference point near the bolt.

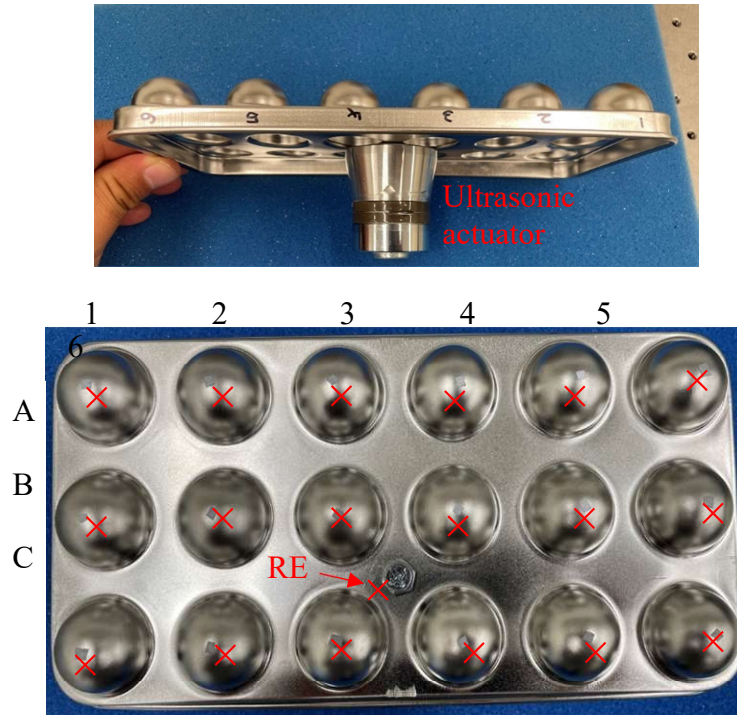


Figure 33: Round ice cube tray with 40 kHz ultrasonic transducer (top), and the measurement points on the front surface

Table 1 Displacement (unit: nm) at the 18 positions with 40 kHz and 5W excitation

	1	2	3	4	5	6	REF
A	49.5	41.8	73.5	40.8	37.2	35.3	170.8
B	74.0	48.9	86.8	75.7	57.2	46.8	
C	32.6	75.6	66.9	28.0	13.5	32.1	

The displacement at the REF point had the largest value. B3, B4, and C4 were close to the ultrasonic transducer; therefore, the displacements of these points were also relatively large compared to other points. However, point C4 had a relatively small displacement, which indicates this point may be close to a nodal point of the mode shape. To study the effect of the excitation power, we measured the displacement at the REF point at five different powers from 5W to 25W. The results are plotted in Figure 34. The displacement had an approximately linear relation with the power levels. Therefore, the displacement measured at a higher power could be calculated with the displacement at a lower power.

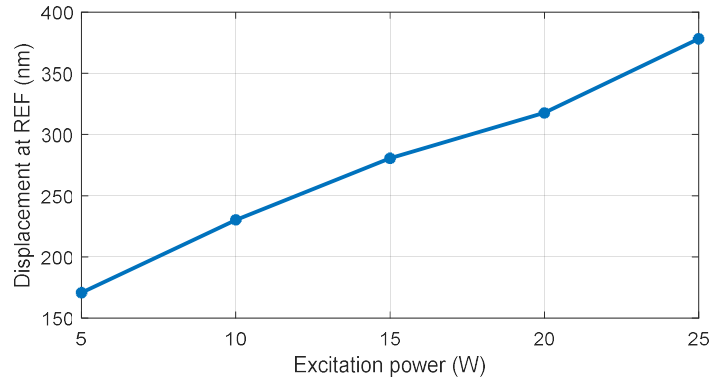


Figure 34: Displacements at the REF excited at five power levels

(b) Commercial ice cube tray

The same test was repeated on an ice cube tray of a commercial ice maker (Figure 35). The ultrasonic actuator was replaced by a PZT plate (Steminc, Inc. SMPL20W15T21R111). The PZT plate was glued at the center position of the top surface of the ice tray with permanent epoxy. First, the working frequency was determined by sweeping the excitation frequency from 20 kHz to 100 kHz. This frequency range was determined by a literature survey. Displacement was measured at 24 locations in Figure 35. The measurement location was placed at the center of each cubic (red cross).

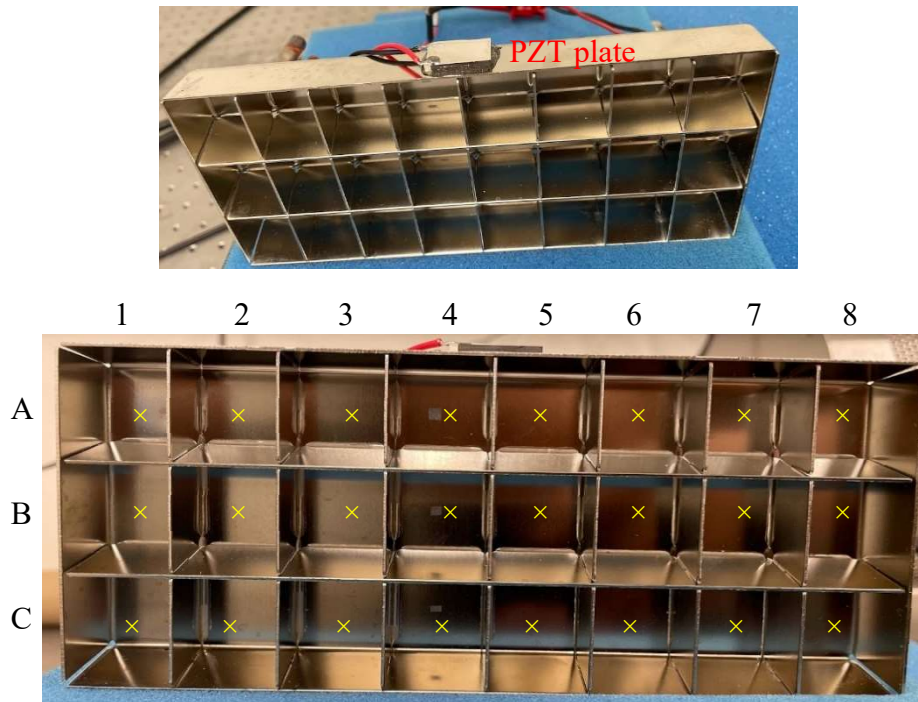


Figure 35: Commercial ice cube tray with a PZT plate (top) and measurement locations (bottom)

Figure 36 plots the displacement responses at C4 when sweeping from 25 kHz to 100 kHz. The peak amplitude is located at 54 kHz. The high amplitude at 25 kHz is caused by the sweeping start frequency and can be ignored here. By checking the displacement responses at A4 and B4, the maximum amplitudes for these two points were also around 54 kHz. Therefore, rest of the tests were conducted at the frequency of 54 kHz.

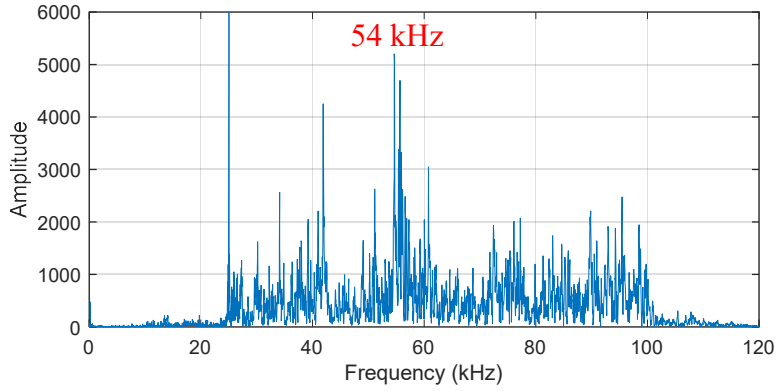


Figure 36: Displacement response at C4 when sweeping from 25 kHz to 100 kHz

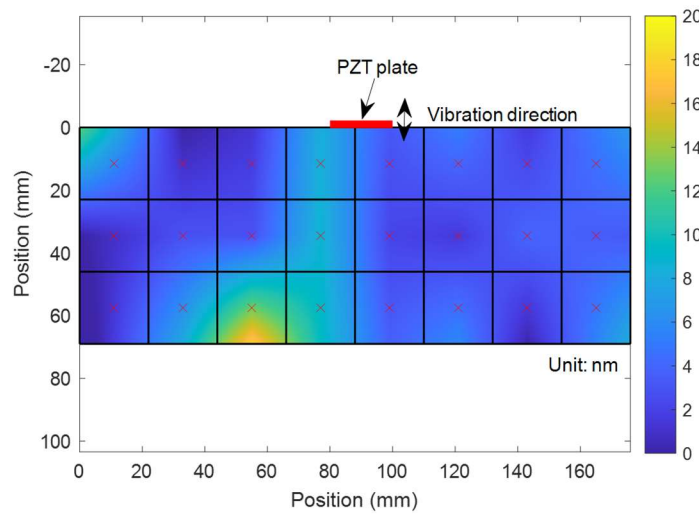


Figure 37: Displacements map for the ice tray with one PZT on the top side surface (excitation frequency: 54 kHz)

Figure 37 shows the displacement map generated using the displacements of the 24 points (red cross locations) with interpolation and extrapolation. The maximum displacement was 12.9 nm at the location of C3, with a minimum displacement of 0.93 nm at B1. We also observed that the three points under the PZT plate, A4, B4, and C4, showed relatively large displacements from 8.4 nm to 9.3 nm. On the ice tray, another two PZT plates of the same type were added to the left and right-side surfaces. The three PZT plates were connected in parallel and excited with the same voltage. Therefore, the output power is three times the power using one PZT plate. The displacement map is shown in Figure 38. The maximum displacement was located at C4 with 69.3 nm, which is 3.8 times the maximum displacement with one PZT. The minimum displacement here was also located at B1 with 3.8 nm, and it is 4.1 times the minimum displacement with one PZT. Therefore, we can conclude that using three PZT plates for excitation is more efficient than using one PZT on the top surface.

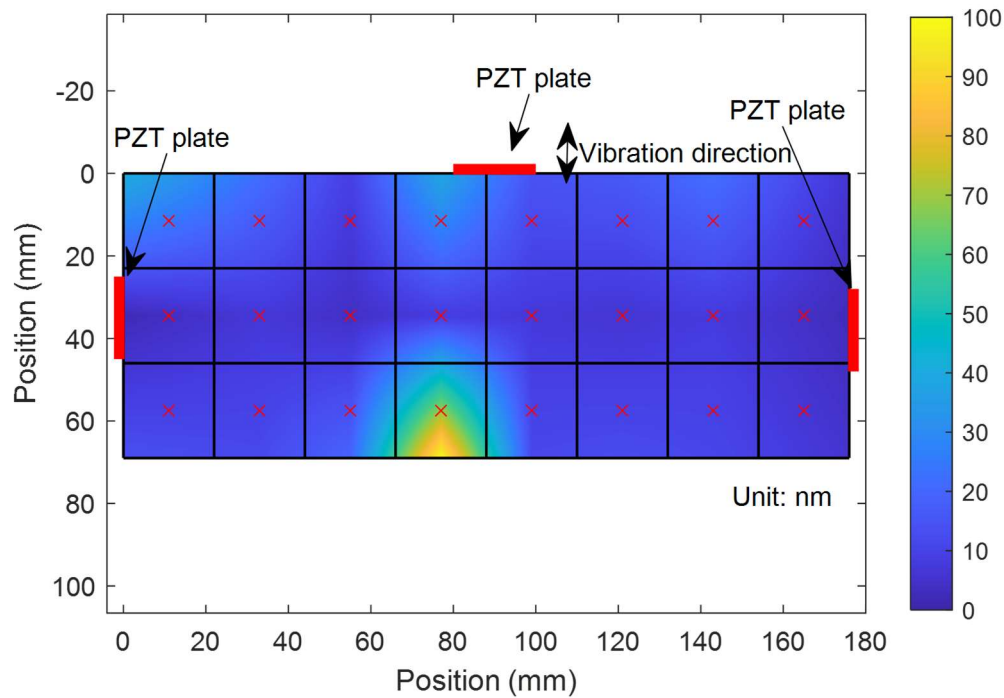


Figure 38: Displacements map for the ice tray with three PZT on the top, left, and right-side surfaces (excitation frequency: 54 kHz).

4.3 Durability Testing

The durability of polymer enhancement of a copper substrate was investigated by conducting thermal cycling tests of a test sample. The sample was subjected to 52 tensile stress tests with a high precision force meter reported above. The freezing temperature for each of the sample was maintained at 7 °F. The adhesion strength during each of these tests is shown in the Figure 39 below. Sample number 1 – 52 are enhanced samples while the last 10 represent bare copper tubes.

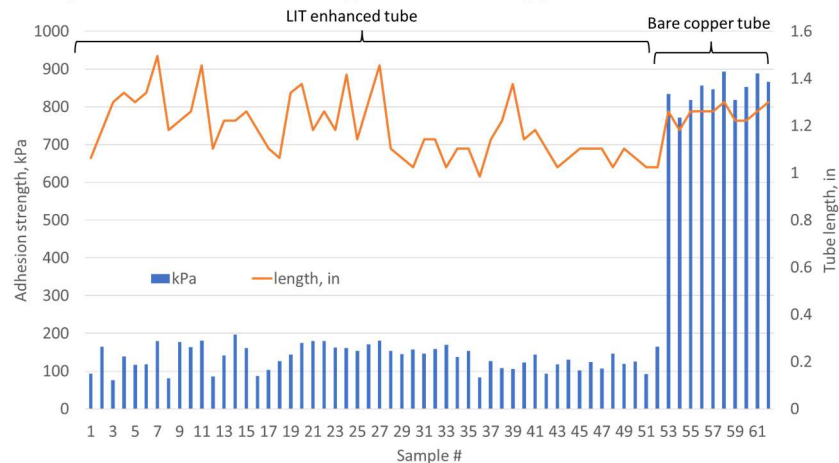


Figure 39: Force measurement on enhanced and as-received copper tubes in contact with ice formed at 7°F

As shown, the overall adhesion strength was significantly lower for the enhanced samples in comparison with the bare copper tube. The enhancement was well preserved even after subjecting to 50+ cycles and no delamination was noticed.

5. CONCLUSIONS

A reliable test methodology and platform was developed. The test platform enabled precise measurement of ice adhesion strength on different materials and geometries representative of ice maker molds employed at all scales in domestic, commercial and industrial applications. The test setup addressed and minimized measurement errors while providing the force necessary to dislodge the ice from a unit surface area of the substrate, at a high resolution. A 50-70% decrease in ice adhesion strength was measured on different materials and geometries investigated. Further, a 40 -53 kHz ultrasonic frequency was found to be effective in dislodging the ice product from the substrate material. Repeated thermal cycling of the enhanced substrate did not show any signs of loss of performance or delamination.